Reciprocal Relations and Proximity of Bases in Flavin–Adenine Dinucleotide*

D. W. Miles† and D. W. Urry

ABSTRACT: The nature of the intramolecular complex of flavin–adenine dinucleotide and the electronic structure of the isoalloxazine chromophore have been investigated using circular dichroism techniques. Seven circular dichroism extrema which are clearly visible in the spectra of flavin mononucleotide and riboflavin at about 450, 370, 340, 307, 265, 235, and 220 mμ are remarkably altered in the interacted state of flavin–adenine dinucleotide. The presence of reciprocal relations in the circular dichroism spectra of flavin–adenine dinucleotide, demonstrated by solvent, pH, and temperature studies, gives strong evidence that the interacted state is substantially populated at low temperature in aqueous solution.

The interbase coupling of several sets of electronic transitions gives rise to regions wherein pairs of circular dichroism bands of opposite sign and almost equal rotational strengths are found. These results are found to be in qualitative accord with recent theoretical studies of the electronic structure of the adenine and isoalloxazine chromophores. A stacked conformation consistent with the analysis and based on the calculations of Song is included for the interacted state of flavin–adenine dinucleotide.

Many physical properties of FAD[1] have been shown to be dependent upon solvent conditions. For example, the addition of a nonpolar solvent such as dioxane or even a polar solvent such as formamide restores the fluorescence and the 500–300-mμ absorption features characteristic of the isoalloxazine chromophore of FMN (Weber, 1966). Similarly the optical rotatory dispersion properties of FAD, which differ significantly from those of FMN in neutral aqueous solution, approximate the sum of the rotations of FMN and AMP in nonaqueous solvents and at low pH (Listowsky *et al.*, 1966; Gascoigne and Radda, 1965; Simpson and Vallee, 1966). These results have been interpreted as evidence that an adenine–isoalloxazine complex is present in pure aqueous solution and that this interaction is abolished at low pH and in nonaqueous solvents. Hypochromism (Whitby, 1953; Warburg and Christian, 1938), photodecomposition (Wada and Sakurai, 1953; Yagi and Ishibashi, 1954), dipole moment and infrared studies (Shikita, 1965), measurements of oxidation–reduction potentials (Koziolo and Knoblock, 1965), and studies of photochemical reactions (Radda and Calvin, 1963; Frisell *et al.*, 1959) have also been found compatible with the reversible stacking of the adenine and isoalloxazine rings. In this communication we present evidence from the circular dichroism spectra for a nonplanar arrangement of the two aromatic systems in close proximity. Positive and negative areas in the circular dichroism spectra of aqueous FAD (which resolve to be nearly equal in area) are found to progressively diminish upon addition of nonaqueous solvents, acid, or upon raising the temperature. This reciprocal behavior of the circular dichroism spectrum is in accord with Tinoco's general theory of optical activity (Tinoco, 1962) and further emphasizes the utility of the concept of reciprocal relations in optical rotation (Urry, 1965, 1968; Miles and Urry, 1967, 1968). Briefly stated this concept is a simplification of the coupled oscillator term of the Tinoco derivation. Because of the $(\nu_\alpha^2 - \nu_\beta^2)^{-1}$ factor in this expression, the interaction of transitions with closely spaced frequencies will often be more important than the other interactions. As an experimental parameter such as solvent, pH, or temperature is varied which brings two different chromophoric groups into juxtaposition, the close-lying transitions may exhibit a coupling in which the circular dichroism peak due to a transition in the first chromophore becomes more positive while the circular dichroism peak of a close-lying electronic transition in the second chromophore becomes more negative in a reciprocal manner.

Experimental Procedure

Circular dichroism measurements were obtained on a Cary Model 60 spectropolarimeter equipped with the Model 6001 circular dichroism attachment. Scan speeds and time constants were chosen to allow sufficient response time and achieve favorable signal-to-noise ratios. The circular dichroism unit was calibrated by using the Cary Model 1401 circular dichroism attachment for the Model 14. The standard used was an aqueous solution of *d*-10-camphorsulfonic acid (J. T. Baker, lot no. 9-361) with an $\epsilon_L - \epsilon_R$ of 2.20 ± 0.05 at 290 mμ. Absorption spectra were run on the Cary Model 14. pH was measured with a Radiometer Model 25SE pH meter.

* From the Institute for Biomedical Research, Education and Research Foundation, American Medical Association, Chicago, Illinois 60610. *Received March 25, 1968.*

† Postdoctoral fellow supported by the Education and Research Foundation of the American Medical Association.

[1] Abbrevations used are listed in *Biochemistry 5*, 1445 (1966).

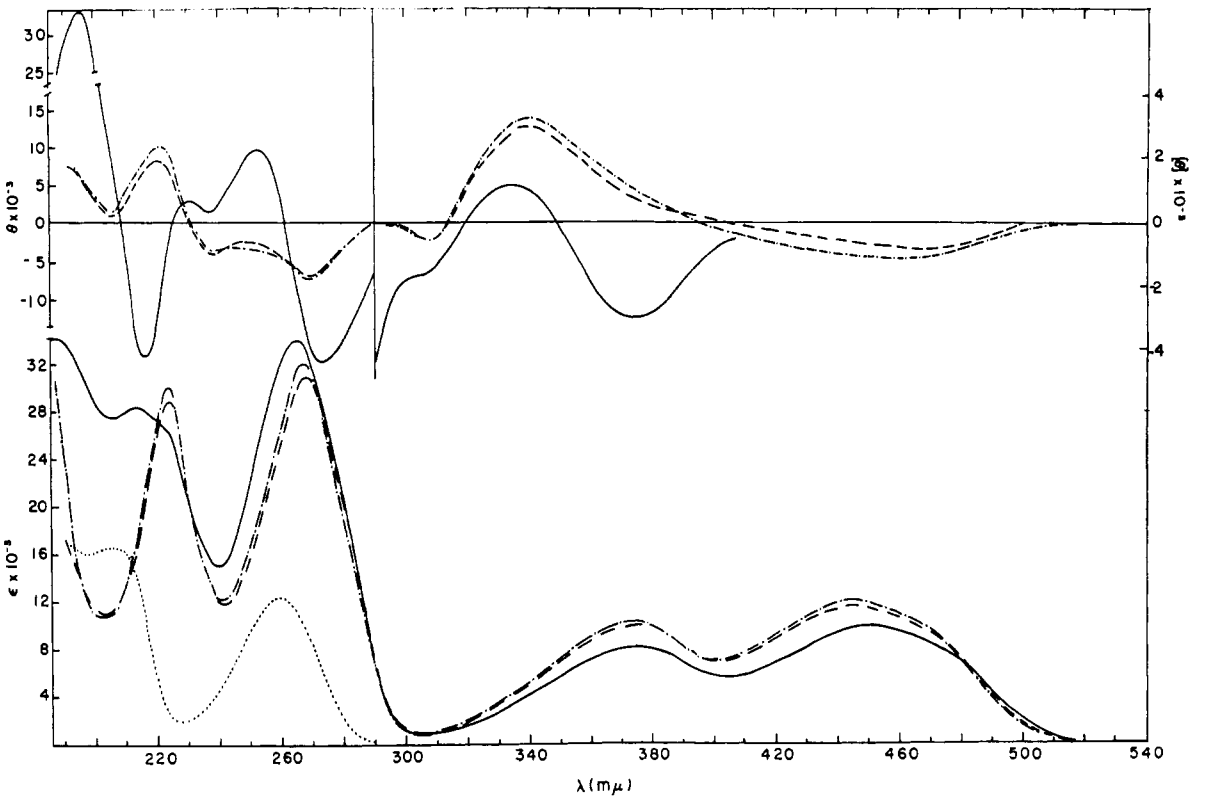

FIGURE 1: Circular dichroism and absorption curves of FAD (——), FMN (- - -), and riboflavin (– · –) in 0.1 M potassium phosphate buffer at pH 7. The absorption curve of AMP at pH 7 (- - - - -) is also given for ready reference. Measurements were made on 1×10^{-4} M solutions. A cell of 2-cm light-path length was used above 300 mμ and a 0.5-cm cell was used for measurements at lower wavelengths.

Sample temperatures were maintained with the Haake KT-62 Kryothermat and were monitored with a YSI Model 42SC telethermometer while spectra were being run. The sample was introduced by means of a syringe and Teflon tubing through a hole drilled in the sample compartment cover with the purpose of eliminating base-line shift arising from the manipulation of the cell compartment carriage. The base line was checked before and after all measurements. As flavin absorbance is high and molar ellipticities relatively low, particularly in the case of FMN and riboflavin, the following test for absorption artifact was conducted. A base line was run with a solvent-filled sample cell and second cell containing a chromate solution in the light beam. The absorbance at the critical wavelengths was 2 or greater. Then the cell containing chromate solution was removed from the light path and the base line was rerun. The test was repeated with an optically active sample with maximum ellipticity of about 40 meg. Absorption artifact was found to be negligible below an absorbance of 2 and less than 1 mdeg at absorbances near 3.

Curve resolution was carried out on the visual DuPont 310 curve resolver. FAD, FMN, riboflavin, and AMP were obtained from Sigma Chemical Co. All solvents were spectral grade except tetramethylurea. All other chemicals were reagent grade.

Results

The circular dichroism and absorption spectra of FAD, FMN, and riboflavin from 500 to 190 mμ are given in Figure 1. The positions of the absorption maxima and circular dichroism maxima of FMN are observed to be virtually identical with the corresponding maxima in riboflavin. Small differences attributable to phosphate–base interactions are found, however, in the magnitudes of the absorption and circular dichroism bands.

The maxima of the Cotton effects of FMN and riboflavin do not always correlate well with the maxima of the absorption spectra which suggests the absorption spectra of the isoalloxazine chromophore is considerably more complex than has previously been supposed. Seven circular dichroism extrema are clearly discernible over the spectral range 500–210 mμ. Riboflavin and FMN exhibit negative extrema at about 450, 307, 265, and 235 mμ and positive extrema at 340 and 220 mμ. The long-wavelength side of the 340-mμ band is perturbed in the 360–380-mμ region by another positive band which is probably related to the 375-mμ absorption maximum of the isoalloxazine chromophore. Similarly the 447-, 265-, and 220-mμ absorption bands of this chromophore can easily be related to the 450-, 265-, and 220-mμ circular dichroism extrema. It is then apparent that the remaining three extrema at 340, 307, and 235 mμ derive from transitions masked in varying degree by more prominent absorption bands. Figure 1 shows that the circular dichroism of FAD is, as expected, significantly different from that of either FMN or AMP, the two moieties which constitute this coenzyme. The

447-mμ absorption band of isoalloxazine exhibits very little optical activity whereas the 370-mμ band (which gives a small positive Cotton effect in FMN and riboflavin) gives a relatively larger Cotton effect in FAD with a negative sign. Positive and negative Cotton effects are observed at about 330 and 300 mμ which most likely arise from the same transitions that gave rise to the 340- and 307-mμ extrema of FMN. The most dramatic differences in the circular dichroism spectra of FAD relative to FMN are found below 300 mμ. In this region two sets of adjacent circular dichroic bands of opposite sign are found in the circular dichroism spectra of FAD. One set of positive and negative areas of rotational strength is found in the 280–240-mμ region with a negative circular dichroism band at 273 mμ and a positive circular dichroism band at 254 mμ. A second pair of bands is found centered around 205 mμ with the maximum of the negative band located at 217 mμ and the positive band peaking at 196 mμ. Another feature of the circular dichroism spectra of FAD below 300 mμ is the small positive circular dichroism band at about 230 mμ. The differences in the absorption spectra of FAD relative to FMN or riboflavin has been discussed in a recent review (Penzer and Radda, 1967).

The effect of adding dioxane to a water solution of FAD is shown in Figure 2. The circular dichroism bands near 273 and 254 mμ are seen to progressively diminish with the addition of dioxane. At 30% dioxane (by volume) the circular dichroism curve of FAD in the 200–220-mμ region resembles the circular dichroism curve of FMN. Figure 2 does not show the effect of dioxane on the circular dichroism spectra above 300 mμ. It is worth mentioning, however, that changes in the circular dichroism spectra in the 280–240-mμ region occur at much lower per cent nonaqueous solvent than the effects in the 500–300-mμ region, that is, we have found that an 80% dioxane (by volume) concentration is required to generate an FMN-like circular dichroism curve for FAD, whereas the effects in the 280–240-mμ region are complete at 30% (by volume) dioxane concentration. The dioxane study suggested a more systematic investigation of the solvent effects in an attempt to define the nature of the forces responsible for the stability of the complex. The importance of the London dispersion forces (induced dipole–induced dipole forces) to the "stacking energy" of the DNA helix (Hanlon, 1966) and dinucleoside phosphates (DeVoe and Tinoco, 1962) and the self-association of various nucleosides (Broom *et al.*, 1967) suggested a comparison of solvent molar refraction and ellipticity of the 273-mμ circular dichroism band. The plot given in Figure 3 demonstrates an approximate linear relationship between ellipticity and molar refraction. These effects are much too large to be accounted for by index of refraction corrections. Similar attempts to relate the reduction in ellipticity in various solvents with the permanent dipole moments or the dielectric constant were unsuccessful.

The effect of increasing temperature is to bring about a gradual decrease in complexity of the circular dichroism pattern (Figure 4) with a simultaneous decrease in magnitude of the 273- and 254-mμ extrema in analogy with the solvent effect (Figure 2). Lowering the pH (Figure 5) brings about a similar reciprocal decrease in the absolute ellipticities of these bands.

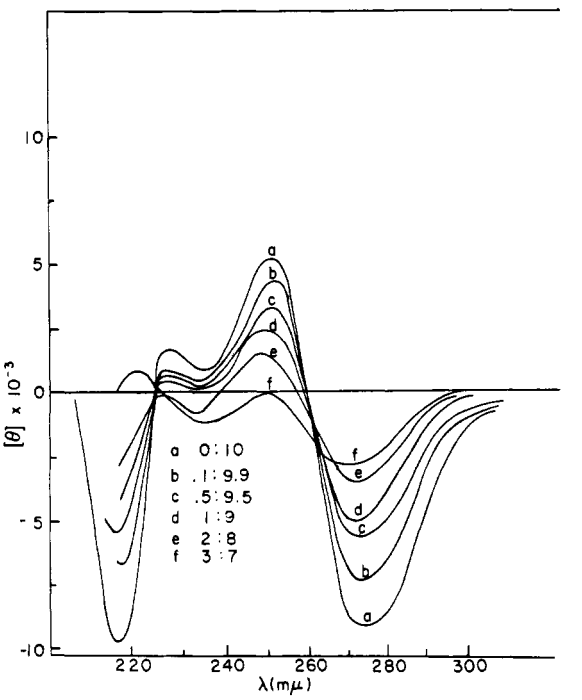

FIGURE 2: Circular dichroism curves of FAD in different water–dioxane mixtures in 0.01 M potassium phosphate buffer at pH 7.

Resolving absorption curves for each chromophore into component bands and then using these bands to describe the interacting FAD system involves the assumption that the frequencies of the transitions are not altered by interactions in the dinucleotide. Because an initial resolution into component bands may not be unique and because of likely shifts on interaction we have chosen to simultaneously fit both the absorption and circular dichroism curves of the interacted FAD system with a minimum of Gaussian functions. Such resolution allows a gross assignment of bands to a given moiety and presents a spectral delineation of dipole strengths and anisotropies which are indicative of types of transitions. It is expected that the reported anisotropies of magnetic transitions will be low, as the procedure associates as much dipole strength as possible with a given rotational strength. The procedure is to fit the circular dichroism curve with a minimum set of Gaussian functions. These functions are then put in the positive mode and their heights are varied in an attempt to fit the absorption curve. One then shifts back and forth between absorption and circular dichroism curves until what appears to be a minimum set of Gaussian functions will simultaneously fit both sets of data by changing only sign and height of the function. As the result of exhaustive attempts three resolutions were obtained which could simultaneously fit the absorption and circular dichroism curves, all resolutions but one gave inverse absorption intensities for the bands resolving near 255 and 264 mμ, that is, assuming the 255-mμ band to be due to an adenine transition and the 269-mμ band to originate in the isoalloxazine moiety only the resolution

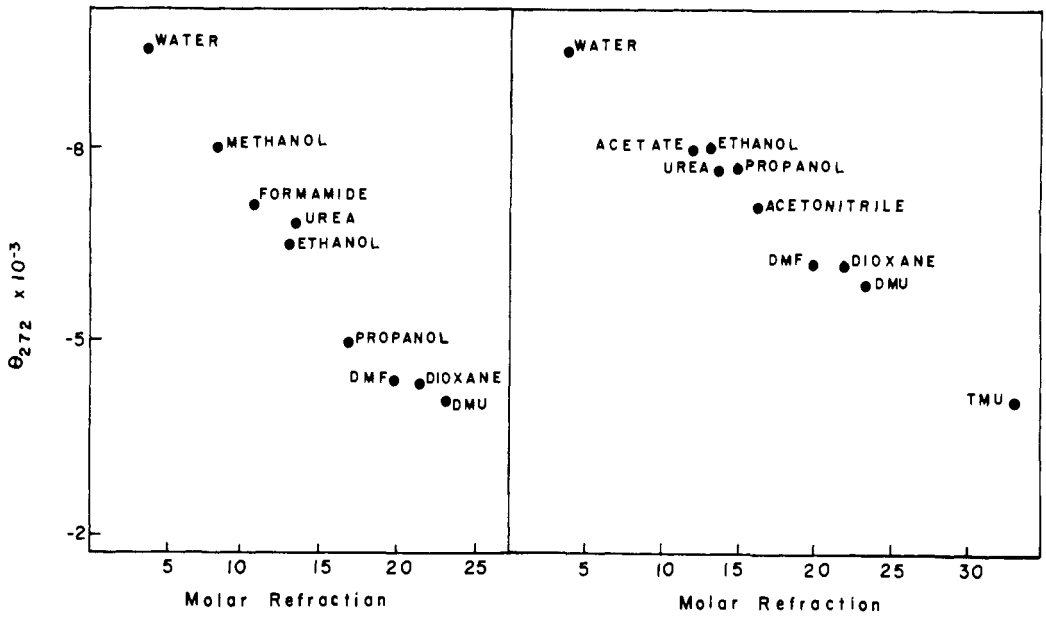

FIGURE 3: Molar ellipticity at 272 mμ plotted as a function of the molar refraction of the nonaqueous component of the water–organic mixtures. Concentrations of the nonaqueous component were 0.025 and 0.05 M for the right and left panels, respectively.

reported in Figures 6 and 7 and in Table I resulted in a less intense 255-mμ absorption. (The other resolutions also required more bands in order to achieve an adequate simultaneous fit.) Bands are resolved at 306, 269, 255, 238, 227, and 214 mμ. The critical values for the resolved Gaussian curves are given in Table I. The background absorption used below 220 mμ in the resolution is considered to contain the second very intense adenine transition (*ca.* 207 mμ in Figure 1). It should be noted that a resolution which simultaneously utilizes absorption and circular dichroism curves will not distinguish between close-lying bands with nearly identical polarizations, or more specifically between bands in which the half-band widths at half-intensity are greater than the separation between band extrema and in which the transition dipole moment directions are almost coincident. In this situation only a single band will be resolved.

Discussion

Spectra. The absorption and circular dichroism spectra and the resolved data taken together allow a more conclusive delineation of the electronic spectrum of flavin than has previously been possible. Even so a resolution cannot be considered unique but rather becomes

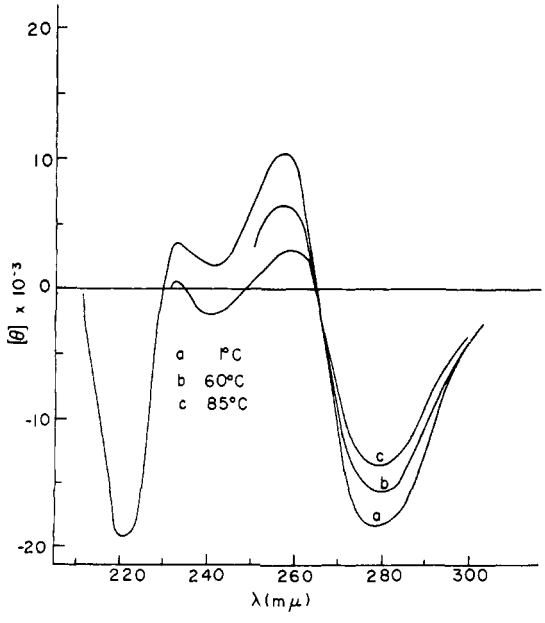

FIGURE 4: Circular dichroism curves of FAD at various temperatures in 0.1 M potassium phosphate buffer at pH 7.

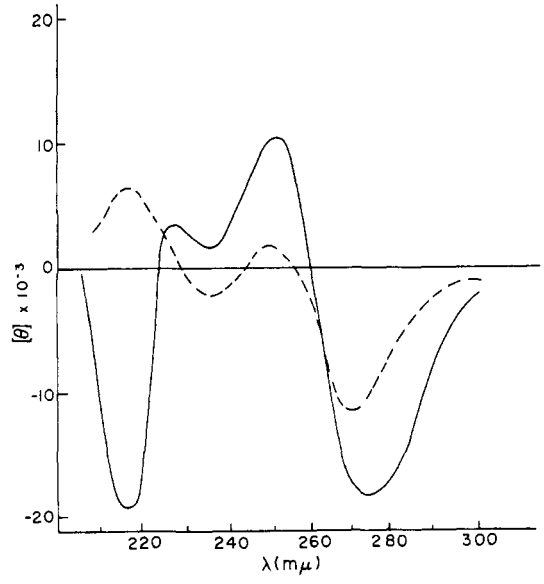

FIGURE 5: Circular dichroism curves of FAD at pH 2.1 (- - -) and 7.0 (—).

TABLE I: Critical Values for Resolved Gaussian Curves of Flavin–Adenine Dinucleotide.

Wavelength of Extremum	Extinction Coef × 10^{-3}	Oscillator Strength	Dipole Strength[a] (D_i) × 10^{36}	Molar Ellipticity × 10^{-3}	Rotational Strength[b] (R_i) × 10^{40}	Anisotropy[c] $\lvert R_i/D_i \rvert$ × 10^4
214 (217)[d]	20.4	0.42 (0.74)[d]	20	−29.0	−21.5	1.07
227 (230)	11.0	0.15 (0.11)	7.42	12.4	6.3 (9)[e]	0.85
238	4.4	0.06	3.43	−11.5	−6.8 (−9)[e]	1.98
255	14.9	0.31	17.6	22.5	20.1 (18)[e]	1.14
269 (271, 275)	23.6	0.40 (0.8)	23.7	−29.8	−22.6 (−18)[e]	0.95
306	0.7	0.006	0.4	−3.06	−1.4	3.5

[a] The dipole strength is calculated from the expression (Moscowitz, 1961), $D_i = 1.63 \times 10^{38}(\epsilon_i \Delta_i/\lambda_i)$, where ϵ^i is the molar extinction coefficient at the curve maximum, λ_i is the wavelength of the ith maximum, and Δ_i is the half-band width at ϵ_i/e. The transition dipole moment μ_i, is $(D)^{1/2}$. [b] The rotational strength is calculated from the expression, $R_i = 1.23 \times 10^{-42}(\theta_i \Delta_i/\lambda_i)$, where θ_i is the molar ellipticity at the maximum of the resolved curve, Δ_i and λ_i are defined above. [c] The significance of anisotropy is discussed by Kauzmann *et al.* (1940). [d] The numbers in parentheses are the theoretically derived values on Song. [e] The calculated rotational strengths for the proposed structure obtained when using the theoretical transition dipole moment directions of Song and the magnitudes from the resolved data (see Appendix).

increasingly credible as it correlates with other data and with *a priori* theoretical calculations. As shown in Figure 1 the absorption spectrum of riboflavin in water consists of four bands centered around 220, 265, 375, and 447 mμ. In the Results section it was observed that there are three Cotton effects in riboflavin near 340, 307, and 235 mμ which do not correspond to maximum in the absorption spectra. The 340-mμ Cotton effect is especially interesting in view of the fact that the fluorescence polarization spectrum has been reported to be constant across the 375-mμ absorption band. These results allowed identification of only one independent electronic transition in this region of the spectrum (Weber, 1966).

The small 307-mμ Cotton effect had been observed in optical rotatory dispersion studies and was attributed to a ketonic absorption band (Simpson and Vallee, 1966). Cotton effects could also arise from n–π^* transitions of the lone-pair electrons on the pyridine-type nitrogens of the isoalloxazine moiety. In either case such transitions are expected to be of low oscillator strength. Accordingly the much less intense n–π^* bands would not introduce an appreciable slope in the polarization ratio on the long-wavelength side of the 375-mμ band. These observations indicate an n–π^* origin for the 340-mμ circular dichroism band. The large anisotropy of the re-

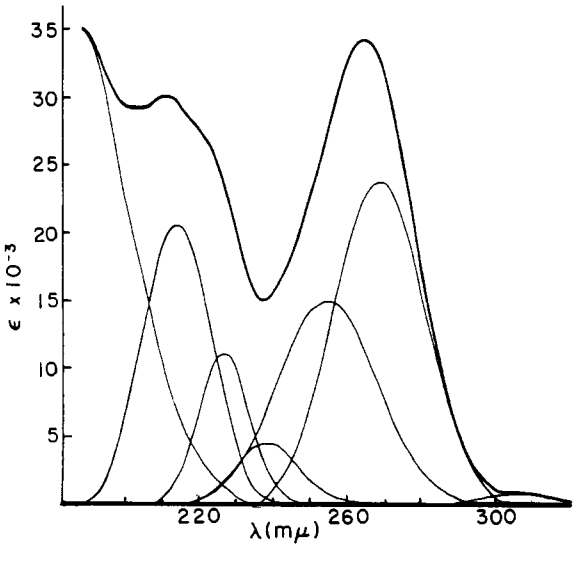

FIGURE 6: The resolved absorption curve of FAD at pH 7 below 300 mμ. Bold-faced curve represents experimental data.

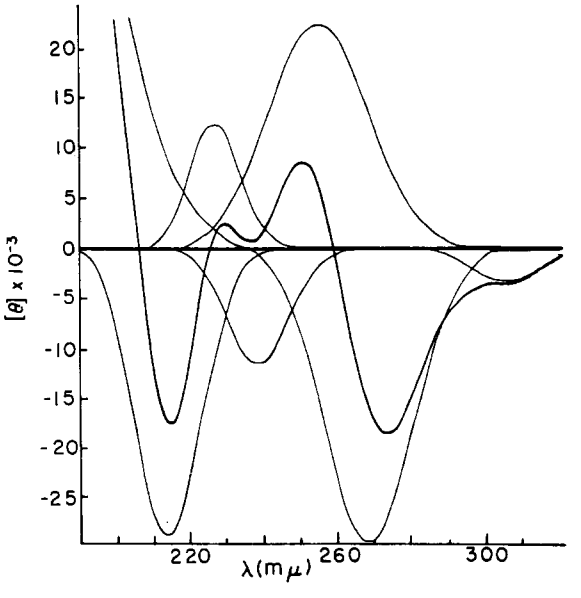

FIGURE 7: The resolved circular dichroism curve of FAD below 300 mμ. Bold-faced curve represents experimental data.

solved 306-mμ band (Table I) demonstrates the large magnetic moment for this transition.

Much work has recently been directed toward interpreting the absorption spectrum of the adenine chromophore. There is substantial evidence that the 260-mμ band is complex containing not only a strong electronic transition at 260 mμ but also a much weaker transition at about 240 mμ. A second strong electronic transition is observed in the spectrum of adenine at 207 mμ (see Figure 1). Comparison of the circular dichroism and absorption bands of FMN and AMP suggest that transitions arising in the isoalloxazine chromophore are found at 220, 235, 265, 307, 340, 375, and 450 mμ and adenine transitions are found at 260, 240, and approximately 207 mμ. The energy of the transition responsible for the 235-mμ circular dichroism extremum in isoalloxazine is subject to the greater uncertainty. Examination of the FMN spectra indicates that the 235-mμ circular dichroism position results from a superposition of the 220-mμ positive band. Hence the true position of this band probably lies several millimicrons to the blue.

It is interesting to compare the energies and intensities of the transitions in the isoalloxazine chromophore as determined by our circular dichroism studies with the recent-all-electron self-consistent field (with configuration interaction) calculations of Song (1968). Song finds strong transitions at 446 ($f = 0.65$), 359 ($f = 0.14$), 275 ($f = 0.59$), 271 ($f = 0.23$), 230 ($f = 0.11$), and 217 mμ ($f = 0.74$). The dipole moments of the 275- and 271-mμ transitions are almost parallel and would therefore appear as a single band in absorption and circular dichroism. The predicted energies are reasonably close to the circular dichroism bands found in FMN with extrema at 450, 265, 235, 220, and a shoulder at about 360 mμ. No π–π^* bands are predicted in the 300–350-mμ region. This is in accord with anisotropies of the bands near 340 and 306 mμ in both FMN and FAD. Making allowances for slight shifts in energy and changes in intensity accruing from strong base–base interaction the comparison of the resolved FAD data (Table I) with Song's results is quite remarkable. It would appear that the day when quantum chemistry can predict the spectral properties of even complex systems is indeed not far off. The calculated values are given in parentheses in Table I.

Reciprocal Relations and the Nature of the Complex. In the absence of steric factors the exchange and dispersion energies are maximal and the surface free energy is minimal when the planar aromatic systems interact in a sandwich or stacked agreement (Sinanoglu and Abdulnur, 1964). A stacked conformation of FAD is also consistent with the observed hypochromism and other physical properties cited in the introduction. This presumed stacked arrangement of FAD is favored in water but becomes unstable with respect to a nonspecified unstacked form as the concentration of organic solvents is increased. Several explanations for the stability of the stacked form in water have recently been reviewed by Penzer and Radda (1967). In the present work the ability of solvents like alcohols and formamide to unstack the aromatic ring systems appears to follow the solvent molar refractivity. Figure 3 shows an almost linear relationship between reduction in the ellipticity at 273 mμ and the molar refraction of the solvent. These results suggest that the London dispersion forces (induced dipole–induced dipole forces) which can be approximated by

$$U_L \cong -\frac{\overline{\quad}9}{8\pi N}\frac{I_a I_b}{I_a + I_b}\frac{R_a R_b}{r_{ab}^6} \qquad (1)$$

are among the principal factors which stabilize the unfolded conformation. In eq 1 the symbols R, I, and N refer to the molar refraction, ionization energy, and Avogadro's number, respectively. The subscripts a and b refer to the nonaqueous component of the solvent and the isoalloxazine or adenine rings, respectively, and r_{ab} is the distance between a and b. In the unstacked conformation each of the aromatic residues is surrounded by a surface of solvent. Dispersion forces between the bases may be considered a principle factor favoring the stacked form (Penzer and Radda, 1967). Accordingly equilibrium between the stacked and unstacked conformation is shifted toward unstacking as the surface of solvent becomes richer in concentration of highly polarizable molecules.

In the coupled oscillator theory of optical rotation, the rotational strength of the α' transition in adenine arises from coupling with all the β transitions in the isoalloxazine chromophore and with all the far-ultraviolet transitions of the sugar and phosphate moieties. When the two aromatic bases are in close proximity the interactions between the bases are favored because of their large dipole strengths and close-lying energies. Therefore when the bases are juxtaposed the rotational strength of the α' transition of adenine is largely the result of coupling with the β transitions in the isoalloxazine moiety. This contribution is written as the following sum

$$R_{\alpha'} = \sum_{\beta} R_{\alpha'\beta} \qquad (2)$$

Similarly the rotational strength of the β' transition in isoalloxazine arises largely from coupling with the α transitions in the adenine moiety and is written as

$$R_{\beta'} = \sum_{\alpha} R_{\beta'\alpha} \qquad (3)$$

The rotational strength of the α' transition in adenine due to coupling with the β' transition in the isoalloxazine chromophore may be written as

$$R_{\alpha'\beta'} = \frac{-2\pi}{c}\frac{V_{\alpha'\beta'}\nu_{\alpha'}\nu_{\beta'}\mathbf{r}_{\alpha'\beta'}\cdot\mu_{\beta'}\mathbf{x}\mu_{\alpha'}}{h(\nu_{\beta'}^2 - \nu_{\alpha'}^2)} \qquad (4)$$

In eq 4, $\mu_{\alpha'}$ and $\mu_{\beta'}$ are the electric dipole moments of transitions α' and β'; $\nu_{\alpha'}$ and $\nu_{\beta'}$ are the transition frequencies; $V_{\alpha'\beta'}$ is the Coulombic energy potential due to interaction of instantaneous charge distributions of the α' and β' transitions; c and h are the speed of light and Planck's constant, respectively. $\mathbf{r}_{\alpha'\beta'}$ is the vector distance between the transition origins. As the numerator does not change sign on interchanging the indices (*i.e.*,

$\mathbf{r}_{\alpha'\beta'} = -\mathbf{r}_{\beta'\alpha'}$ and $\mu_{\beta'}\mathbf{x}\mu_{\alpha'} = -\mu_{\alpha'}\mathbf{x}\mu_{\beta'}$) while the the denominator does, it is apparent that the rotational strength of the β' transition in isoalloxazine which derives from coupling with the α' transition in adenine is the same value but opposite in sign, *i.e.*

$$R_{\alpha'\beta'} = -R_{\beta'\alpha'} \tag{5}$$

Thus they are seen to vary in a reciprocal manner. In favorable circumstances where the α' and β' transitions have relative orientations giving rise to large values for the triple-scalar product, $\mathbf{r}_{\alpha'\beta'}\cdot\mu_{\beta'}\mathbf{x}\mu_{\alpha'}$, and have closely spaced energies such that

$$(\nu_{\beta'}^2 - \nu_{\alpha'}^2)^{-1} \tag{6}$$

is large, then it is expected that these transitions will derive a substantial part of their rotational strength from coupling one with the other when in a stacked conformation. In the case of FAD it is significant to point out that the resolved bands can be grouped into three pairs (see Table I and Figures 1, 6, and 7) the 269- and 255-mμ bands, the 238- and 227-mμ bands, and the 214- and 196-mμ bands. The rotational strengths of the first two pairs are of approximately equal magnitude but opposite signs. As demonstrated in Figures 2, 4, and 5 this complexity can be largely removed by nonaqueous solvents, pH, and by raising the temperature. Hence as the two aromatic ring systems are brought together by varying the temperature, solvent, or pH, one finds that the ellipticities of these pairs of coupled transitions increase in a reciprocal manner.

The specific nonplanar arrangement of the two aromatic systems which gives rise to the observed reciprocal behavior can be described once an assignment of the transitions has been made and the transition moment directions are fixed with respect to the molecular framework. A structure dependent upon theoretical work on the electronic structures of the adenine (Berthod *et al.*, 1967) and isoalloxazine (Song, 1968) chromophores and derived from the observed coupling of the 269- and 255-mμ bands and the oppositely signed 238- and 227-mμ bands and 214- and 196-mμ bands is indicated in Figure 8. In this conformation the angle between pairs of transitions is large giving large values for the triple-scalar product, $\mathbf{r}_{\alpha'\beta'}\cdot\mu_{\beta'}\mathbf{x}\mu_{\alpha'}$, for each pairwise coupling. Moreover interactions between nonadjacent bands, such as the 255-mμ adenine–217-mμ isoalloxazine band and the 271-mμ isoalloxazine–205-mμ adenine bands, would be small as the transition moments of these combinations are almost parallel. Also μ_{238} and μ_{227} are small (see Table I, footnote *a*).

In Appendix A it is found that the circular dichroism spectrum calculated for the proposed structure of Figure 8 yields rotational strengths for the first two sets of bands which are of the same sign and same order of magnitude as those found by the simultaneous resolution of the circular dichroism and absorption spectra (Table I). The calculations in the Appendix are based on the dipole–dipole approximation for $V_{\alpha'\beta'}$. As no experimental results have been reported to date for the

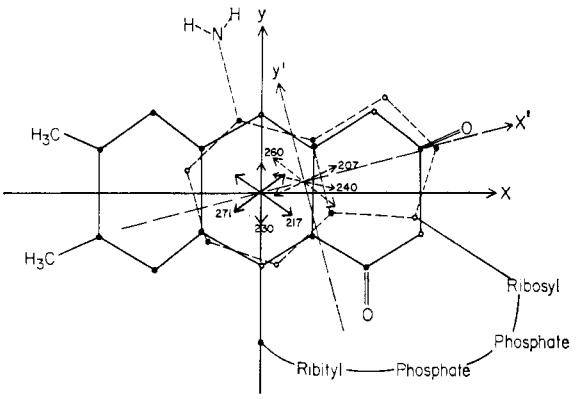

FIGURE 8: Considered structure for a stacked conformation of FAD. The essential statement of the indicated stacking is the angle made by the planar projection of the x and x' axes. Translation of either base may occur along its long axis. The adenine moiety (dashed structure) underlies the isoalloxazine moiety (solid line). Directions of transition moments are similarly indicated. Open circles indicate nitrogens.

isoalloxazine chromophore, the proposed structure is of course dependent upon the ability of theoretical studies to predict transition moment directions. There is, however, reason for guarded optimism regarding the ability of the more sophisticated self-consistent field with configuration interaction treatments (particularly those which also include the σ electrons) to predict transition moment directions. A recent self-consistent field with configuration interaction treatment on uracil (O. W. Adams, private communication) predicts that the polarization of the characteristic 260-mμ transition of uracil is at 20° measured counterclockwise from the C_4–N_1 line. Experimentally the 260-mμ band of 1-methylthymine is polarized at 19 ± 3° and that of 9-methyladenine is polarized at either −3 or 45 ± 3° measured counterclockwise from the C_4–C_5 line (Stewart and Davidson, 1963, 1964; Stewart and Jensen, 1964). Berthod's self-consistent field with configuration interaction treatment of adenine and uracil (Berthod *et al.*, 1967) places the 260-mμ bands at 37 and 10°, respectively. Insofar as the experiments on 1-methylthymine and 9-methyladenine are representative of the situation in uracil and adenine, the theoretical results are very satisfactory.

The calculated rotational strengths for a considered structure (see Appendix A) are reported in Table I (see footnote *e*). It is seen that both the proper sign and correct order of magnitude are obtained for the first two sets of bands. The pair of bands at shorter wavelengths which are incompletely resolved also give the correct signs. The observed reciprocal relations, the resolution which compared favorably with Song's independent calculations and particularly the very limiting constraints imposed by the three pairwise couplings of transitions, which are so adequately met, are the basis for the stacked conformation given in Figure 8.

In the calculation a distance of 4.5 Å was used. It may be that the distance is closer to 3.5 Å in which case the calculated values would be larger. While decreasing

TABLE II

Adenine	Isoalloxazine
$\mathbf{e}_{260} = -0.64\mathbf{i} + 0.77\mathbf{j}$	$\mathbf{e}_{271} = \mathbf{e}_{275} = -0.77\mathbf{i} - 0.64\mathbf{j}$
$\mathbf{e}_{240} = 0.98\mathbf{i} - 0.18\mathbf{j}$	$\mathbf{e}_{230} = -1.0\mathbf{j}$
$\mathbf{e}_{207} = 0.86\mathbf{i} + 0.50\mathbf{j}$	$\mathbf{e}_{217} = 0.80\mathbf{i} - 0.60\mathbf{j}$

the distance would result in larger values the inclusion of damping factors would lower the calculated result. It is, in fact, surprising that eq 4 does so well considering the extent of overlap of the resolved bands (Figure 6) and the equation's expected limited range of application. Approximate retention of the band characteristics of the noninteracted chromophores and dominance of coupling between the two closest energy transitions are features which have been observed in both the FAD and adenosine 5′-mononicotinate (Miles and Urry, 1967). These observations, which extend beyond the validity of eq 4, experimentally demonstrate the utility of the concept of reciprocal relations in assessing proximity of chromophoric moieties with close-lying transition energies.

Appendix A

In order to calculate the rotational strength of the FAD transitions from eq 4, a method of approximating the potential, $V_{\alpha'\beta'}$, of the interaction of the instantaneous charge distribution of the groups must be decided upon. Assuming the dipole approximation to the multipole expansion of $V_{\alpha'\beta'}$, eq 4 becomes (Tinoco, 1962)

$$R_{\alpha'\beta'} = -\frac{2\pi\nu_{\alpha'}\nu_{\beta'}|\mu_{\alpha'}||\mu_{\beta'}|}{ch(\nu_{\beta'}^2 - \nu_{\alpha'}^2)}GF$$

$$GF = \left[\mathbf{e}_{\alpha'}\cdot\mathbf{e}_{\beta'} - \frac{3}{|\mathbf{r}_{\alpha'\beta'}|^2}(\mathbf{e}_{\alpha'}\cdot\mathbf{r}_{\alpha'\beta'})(\mathbf{e}_{\beta'}\cdot\mathbf{r}_{\alpha'\beta'})\right] \times \frac{\mathbf{e}_{\beta'}\mathbf{x}\mathbf{e}_{\alpha'}\cdot\mathbf{r}_{\alpha'\beta'}}{|\mathbf{r}_{\alpha'\beta'}|^3}$$

where the e's are unit vectors in the direction of the appropriate transition moment vector and all other symbols are as previously defined. Values for the frequencies and transition moments are obtained from the data of Table I with the exception of the 207-mμ adenine transition. The e vectors are determined from the theoretical work of Song and Pullman as discussed in the text and are listed in Table II in terms of the unprimed coordinate system of Figure 8. The magnitude of the 207-mμ adenine transition moment is 4 D (DeVoe and Tinoco, 1962). The distance vector, $\mathbf{r}_{\alpha'\beta'}$, in eq 4-A is given by the expression $\mathbf{r}_{\alpha'\beta'} = x'\cos\phi\,\mathbf{i} + x'\sin\theta\,\mathbf{j} + z\mathbf{k}$, where x' is the projection of the center of the adenine chromophore along the x' axis and ϕ is the angle made by the planar projection of the x and x' axis. The essential statement of the proposed structure is the angle ϕ. Translation may occur along the x' axis. Thus the value of x' in the above expression as well as the vertical distance, z, are not specified in the proposed structure. Calculations based on the geometry given in Figure 8, *i.e.*, $x' = 0.7$ Å and $= 15°$, and the assumption that the vertical distance between the chromophores is 4.5 Å gives calculated rotational strengths for the resolved Cotton effects in the 300–195-mμ region of the right sign and right order of magnitude.

Acknowledgment

The authors wish to thank D. J. Caldwell for helpful discussions and A. Ruiter for technical assistance.

References

Berthod, H., Giessner-Prettre, E., and Pullman, A. (1967), *Intern. J. Quan. Chem. 1*, 123.
Broom, A. D., Schweizer, M. P., and Ts'o, P. O. P. (1967), *J. Am. Chem. Soc. 89*, 3612.
DeVoe, H., and Tinoco, I., Jr. (1962), *J. Mol. Biol. 4*, 500.
Frisell, W. R., Chung, C. W., and Mackenzie, C. G. (1959), *J. Biol. Chem. 234*, 1297.
Gascoigne, I. M., and Radda, G. K. (1965), *Chem. Commun.* 534.
Hanlon, S. (1966), *Biochem. Biophys. Res. Commun. 23*, 861.
Kauzmann, W. J., Walter, J. E., and Eyring, H. O. (1940), *Chem. Rev. 26*, 339.
Koziolo, J., and Knoblock, E. (1965), *Biochim. Biophys. Acta 102*, 289.
Listowsky, I., Englard, S., Betheil, J., and Seifter, S. (1966), *Biochemistry 5*, 2548.
Miles, D. W., and Urry, D. W. (1967), *J. Phys. Chem. 71*, 4448.
Miles, D. W., and Urry, D. W. (1968), *J. Biol. Chem.* (in press).
Moscowitz, A. (1961), *in* Optical Rotatory Dispersion, Djerassi, C., Ed., New York, N. Y., McGraw-Hill, p 150.
Penzer, G. R., and Radda, G. K. (1967), *Quart. Rev. (London)*, 43.
Radda, G. K., and Calvin, M. (1963), *Nature 200*, 464.
Shikita, T. (1965), *Med. J. Osaka Univ. 8*, 365.
Simpson, R. T., and Vallee, B. L. (1966), *Biochem. Biophys. Res. Commun. 22*, 712.
Sinanoglu, O., and Abdulnur, S. (1964), *Photochem. Photobiol. 3*, 333.
Song, P.-S. (1968), *Ann. N. Y. Acad. Sci.* (in press).
Stewart, R. F., and Davidson, N. (1963), *J. Chem. Phys. 39*, 255.
Stewart, R. F., and Davidson, N. (1964), *Biopolymers Symp. 1*, 465.
Stewart, R. F., and Jensen, L. H. (1964), *J. Chem. Phys. 40*, 2071.
Tinoco, I., Jr. (1962), *Advan. Chem. Phys. 4*, 113.
Urry, D. W. (1965), *Proc. Natl. Acad. Sci. U. S. 54*, 640.

Urry, D. W. (1968), *Ann. Rev. Phys. Chem.* (in press).
Wada, T., and Sakurai, Y. (1953), *J. Japan Soc. Food Nutr. 5*, 44.
Warburg, O., and Christian, W. (1938), *Biochem. Z. 296*, 294.
Weber, G. (1966), Flavines and Flavoproteins, Slater, E. C., and Veeger, C., Ed., Amsterdam, Elsevier.
Whitby, L. G. (1953), *Biochem. J. 54*, 437.
Yagi, K., and Ishibashi, I. N. (1954), *Vitamins (Kyoto) 7*, 935.

Transfer Ribonucleic Acids in *Escherichia coli*. Multiplicity and Variation*

Karl H. Muench† and P. Alicia Safille

ABSTRACT: Gradient partition chromatography of transfer ribonucleic acid from *Escherichia coli*, strain B, reveals 56 transfer ribonucleic acid chains for 20 amino acids. Acceptor profiles, determined with partially purified aminoacyl transfer ribonucleic acid synthetases, demonstrate three transfer ribonucleic acids for asparagine, cysteine, glycine, histidine, and threonine; four transfer ribonucleic acids for proline, and five transfer ribonucleic acids for tryptophan. Each of the tryptophan transfer ribonucleic acid can exist in an active and an inactive conformation as measured by response to chloroquine in the charging medium. Although asparagine transfer ribonucleic acids and aspartic acid transfer ribonucleic acid emerge in the same region of the profile, asparagine and aspartic acid do not share common acceptors, as shown by studies involving periodate oxidation. The profiles of leucine and tyrosine acceptor are essentially constant for different lots of transfer ribonucleic acid prepared from commercial cells, whereas the acceptor profiles for eight other amino acids vary markedly. The variability is not explainable by differential extraction or artifacts in resolution.

Various techniques of separation (RajBhandary and Stuart, 1966) have revealed multiple tRNAs (isoacceptors) for most of the amino acids. As techniques have improved and multiplied, so has the recorded multiplicity of tRNA expanded. The general validity of this multiplicity is accepted. However, the reasons for multiplicity are incompletely understood. Even less understood are reasons for variable amounts of isoacceptors and for changes in those amounts. To establish the minimum number of tRNAs and the isoacceptor constancy in *Escherichia coli*, we examined four lots of tRNA by gradient partition chromatography. For 7 amino acids not previously studied (Muench and Berg, 1966a) 24 tRNAs were found, bringing the number of tRNAs for 20 amino acids to at least 56. At least two tRNAs have been resolved for each amino acid, five for leucine and tryptophan. Relative amounts of isoacceptors varied widely in some cases and were constant in others.

Experimental Procedures

Materials. E. coli strain B cells were purchased from Grain Processing Corp., Muscatine, Iowa.

Lots 1 and 4 of tRNA were prepared in our laboratory as described (Muench and Berg, 1966a) from two different batches of the commercial cells stated to be grown in minimal[1] medium and harvested in exponential phase at three-fourths maximal growth. Lots 2 and 3 were prepared by Schwarz BioResearch (6701 and 6603, respectively) by the method of Gutcho (1968) from cells also supplied by Grain Processing Corp. but stated to be grown in enriched[1] medium and harvested in exponential phase at three-fourths maximal growth. Lot 2 was derived from several batches of cells, whereas lot 3 was derived from one batch (S. Gutcho, personal communication).

Pure tyrosyl-tRNA synthetase (Calendar and Berg, 1966) was a gift from Dr. R. Calendar. Other aminoacyl-tRNA synthetases were prepared by batch fractionation

* From the Departments of Medicine and Biochemistry, University of Miami School of Medicine, Miami, Florida. *Received April 15, 1968.*

† Faculty Research Associate, American Cancer Society. Supported by Grants NIH-AM-09001-04 and NIH-5-T0I-AM-5472-03 from the National Institutes of Health, U. S. Public Health Service, and ACS-PHA-21 from the American Cancer Society.

[1] According to the Grain Processing Corp., "minimal" medium consists of 1.0% glucose, 1.0% yeast extract, 2.08% K_2HPO_4, and 1.62% KH_2PO_4; "enriched" medium consists of 4.0% peptone casamino acids, 1% glucose, 0.5% yeast extract, 0.64% K_2HPO_4, 0.04% $(NH_4)_2HPO_4$, 0.003% KCl, 0.001% each of $MgSO_4$, $CaCl_2$, and $ZnSO_4$, and 0.008% $FeCl_3$.